Chemical Synthesis

Research Article

High-silica KFI zeolite: highly efficient synthesis and catalysis in methanol amination reaction

Rui Wu[1,#], Jinfeng Han[1,#], Jing Li[2], Lin Li[3], Shuang Liu[1], Peng Tian[4,*], Wenfu Yan[1,*] iD

[1]State Key Laboratory of Inorganic Synthesis and Preparative Chemistry, College of Chemistry, Jilin University, 2699 Qianjin Street, Changchun 130012, Jilin, China.
[2]College of Petrochemical Technology, Jilin Institute of Chemical Technology, 45 Chengde Street, Jilin 132012, Jilin, China.
[3]College of Chemistry, Tianjin Normal University, 393 Binshui West Road, Tianjin 300387, China.
[4]National Engineering Research Center of Lower-Carbon Catalysis Technology, Dalian Institute of Chemical Physics, Chinese Academy of Sciences, 457 Zhongshan Road, Dalian 116023, Liaoning, China.
[#]Authors contributed equally.

[*]**Correspondence to:** Prof. Wenfu Yan, State Key Laboratory of Inorganic Synthesis and Preparative Chemistry, College of Chemistry, Jilin University, 2699 Qianjin Street, Changchun 130012, Jilin, China. E-mail: yanw@jlu.edu.cn; Prof. Peng Tian, National Engineering Research Center of Lower-Carbon Catalysis Technology, Dalian Institute of Chemical Physics, Chinese Academy of Sciences, 457 Zhongshan Road, Dalian 116023, Liaoning, China. E-mail: tianpeng@dicp.ac.cn

Abstract

The hydrogen form of low-silica **KFI** zeolite, with a Si/Al ratio of 3.2 (referred to as H-KFI-3.2), has been shown to possess significant selectivity for monomethylamine (MMA) and dimethylamine (DMA) in methanol amination reactions. However, its industrial viability for MMA and DMA synthesis has been hindered by its relatively low methanol (MeOH) conversion and yield of MMA plus DMA. In this study, we synthesize high-silica **KFI** zeolite with an elevated framework Si/Al ratio of 5.4 (designated as KFI-5.4) using a novel K$^+$ and 18-crown-6 complex [referred to as (K$^+$)CCH, with a ratio of 18-crown-6 to K$^+$ of 2.85] as an organic structure-directing agent. Control experiments have demonstrated that the presence of both K$^+$ and OH$^-$ ions is essential for the formation of KFI-5.4 zeolite. The hydrogen form of KFI-5.4 (H-KFI-5.4) exhibits significantly enhanced MeOH conversion (95.2%) and yield (75.1%) of MMA plus DMA compared to the low-silica H-KFI-3.2 under similar reaction conditions. This represents the highest level of catalytic performance among reported small-pore zeolites to date. Furthermore, the yield and selectivity of MMA plus DMA can be further improved by modifying KFI-5.4 with an appropriate loading of Na$^+$, which suppresses the formation of the by-product dimethyl ether. This study introduces a new high-silica **KFI** zeolite catalyst with exceptional MeOH conversion and yield for the production of MMA plus DMA.

Keywords: K$^+$ and 18-crown-6 complex hydroxide, high-silica KFI zeolite, methylamine synthesis, metal modification

INTRODUCTION

Monomethylamine (MMA, 3.7 Å × 3.9 Å × 4.4 Å) and dimethylamine (DMA, 3.9 Å × 4.7 Å × 6.0 Å) are versatile chemicals used in producing surfactants, dyestuffs, solvents, pharmaceuticals, insecticides, and more[1-4]. Presently, the predominant method for synthesizing MMA and DMA involves the reaction of methanol (MeOH) and ammonia (NH_3) using amorphous silica-alumina catalysts. However, this process yields a significant amount of thermodynamically favorable yet less desirable trimethylamine (TMA, 3.9 Å × 5.4 Å × 6.1 Å) and the by-product dimethyl ether (DME)[5]. Thus, there is a compelling need to develop shape-selective catalysts that can achieve high yields of MMA and DMA while minimizing the formation of TMA and DME[6].

Zeolite materials have emerged as promising candidates for this purpose owing to their molecular sieving capability and adjustable acid properties. For instance, large-pore **MOR** zeolite with a 12-membered-ring window of 6.5 Å × 7.0 Å was commercially utilized in methylamines (MAs) production during the 1980s[7]. However, a pore-size-reduction post-treatment was necessary to enhance the yield of MMA plus DMA. Subsequently, small-pore zeolites, such as **KFI**[8], H-rho (**RHO**)[9], H-PST-29 (**PWN**)[9], DNL-6 (**RHO**)[10], and SAPO-34 (**CHA**)[11], were discovered to exhibit superior shape selectivity for MMA and DMA due to their smaller pore sizes (3.0 Å ~ 4.5 Å), which restricted the exit of TMA. Among these small-pore zeolites, **KFI** zeolite stands out as one of the most promising catalysts for MMA and DMA synthesis.

KFI zeolite, with a pore size of 3.9 Å × 3.9 Å, is structured from an alternating sequence of α-cage and γ-cage[12]. Various methods have been developed for synthesizing **KFI** zeolite with different Si/Al ratios. In 1948, **KFI** zeolite with a Si/Al ratio of 2.0 was first synthesized through the hydrothermal conversion of synthetic and natural analcites or leucites[13]. Subsequently, ZK-5 type zeolites with **KFI** framework topology possessing expanded Si/Al ratios ranging from 1.23 to 4.7 have been synthesized in the presence of organic structure-directing agents (OSDAs), such as N, N'-dimethyltriethylenediammonium cation[14], 18-crown-6[15], and tetramethylammonium hydroxide[16]. To reduce the cost and pollution associated with the calcination of as-synthesized material, OSDA-free methods were investigated widely, involving the introduction of K^+ along with other cations as inorganic structure-directing agents[17-20]. For instance, **KFI** zeolite with a Si/Al ratio of 3.8 was synthesized using K^+ and Sr^{2+}[17], while a Si/Al ratio of 3.1 was achieved for **KFI** zeolite employing K^+ and Cs^+ as inorganic structure-directing agents[18].

In addition to direct synthesis, **KFI** zeolite can also be synthesized via the interzeolite transformation of zeolite Y with the assistance of K^+, Na^+, and Cs^+, resulting in a Si/Al ratio of 3.0~4.8[19,20]. Recently, it was reported that a high Si/Al ratio of 5.0 [determined by nuclear magnetic resonance (NMR) analysis] was achieved for the **KFI** framework only in the presence of K^+, albeit requiring a prolonged crystallization time of ten days at 150 °C or 15 days at 140 °C[21]. However, synthesizing **KFI** zeolite with a framework Si/Al ratio higher than 5.0 remains a challenge. According to the charge balance principle, introducing a structure-directing agent with lower charge density might increase the Si/Al ratio of the resulting zeolites[22].

Our previous study revealed that H-KFI zeolite with a Si/Al ratio of 3.2 (referred to as H-KFI-3.2) exhibited a remarkable selectivity of 94.4% for MMA plus DMA in MA products under reaction conditions of 350 °C, a weight hourly space velocity of MeOH ($WHSV_{MeOH}$) = 0.813 h^{-1}, and NH_3/MeOH = 2.0[8]. However, the corresponding yield (54.7%) was low due to the relatively low MeOH conversion of 63.4%. Furthermore, it was suggested that increasing the Si/Al ratio of the zeolite could effectively enhance the yield of MMA plus DMA by improving MeOH conversion[9,23]. For instance, raising the Si/Al ratio of hydrogen form **RHO**

zeolite (H-rho) and **PWN** zeolite (H-PST-29) led to increased MeOH conversion and, subsequently, higher yields of MMA plus DMA[9]. Additionally, it was demonstrated that a higher Si/Al ratio for (H)Al-RUB-41 (framework type **RRO**) zeolite, possessing stronger acid sites, resulted in higher MeOH conversion and yield of MMA plus DMA[23]. Therefore, increasing the Si/Al ratio of **KFI** zeolite is highly desirable for its further applications in MMA and DMA synthesis.

Unfortunately, increasing the Si/Al ratio of zeolite tends to decrease the selectivity of MMA plus DMA. For instance, elevating the Si/Al ratio of HMOR zeolite (**MOR**) from 5 to 7.5 decreased MMA plus DMA selectivity from 72.2% to 50.4%[24]. It is noteworthy that Na^+ loading of mordenite (**MOR**) can enhance the selectivity of MMA plus DMA due to several factors, including suitable shape selectivity and acid strength, disruption of the H-bond network of methanol agglomerates and open dimers, and weaker adsorption of MMA[25]. This observation aligns with experimental results obtained by Zhang *et al.*, where Na^+ loading of HMOR increased MMA plus DMA selectivity from 61.3% to 69.9%[26]. Thus, exploring the impact of Na^+ loading on the catalytic performance of zeolites is essential for developing high-performance catalysts in MMA and DMA synthesis.

In this study, we present the synthesis of **KFI** zeolite (KFI-5.4) with the highest framework Si/Al ratio recorded to date at 5.4 (determined via NMR analysis). This achievement was realized by employing a novel OSDA comprising an 18-crown-6 and K^+ complex, with an 18-crown-6/K^+ ratio of 2.85. The resulting H-KFI-5.4 exhibited exceptional MeOH conversion (95.2%) and yield (75.1%) for MMA plus DMA, representing the pinnacle of catalytic performance among small-pore zeolites reported thus far. Additionally, we investigated the impact of modifying KFI-5.4 zeolite with varying Na^+ loadings on MA synthesis, laying the groundwork for enhancing the yield and selectivity of MMA plus DMA through zeolite catalysts.

EXPERIMENTAL
Materials and chemicals
Potassium hydroxide (Aladdin, 99.99%) and 18-crown-6 (Energy Chemical, 99%) were employed in the preparation of (K^+)CCH. Sodium aluminate (Sinopharm Chemical Reagent, Al_2O_3 ≥ 41.0%) and Ludox AS-40 (Sigma-Aldrich, 40 wt.%, suspension in water) were utilized for synthesizing KFI-5.4 zeolite in the presence of low-silica **KFI** zeolite (Si/Al = 3.8, denoted as KFI-3.8) seed and (K^+)CCH. The low-silica KFI-3.8 zeolite seed was synthesized following our previous work[8], and detailed experimental procedures are provided in the Supplementary Materials. Ammonium chloride (Tianjin Fuchen Chemical Reagent Co., Ltd., NH4Cl ≥ 99.5%) and sodium chloride (Tianjin Xinbote Chemical Co., Ltd., NaCl ≥ 99.5%) were used in the preparation of Na^+-modified KFI-5.4 zeolite. Additionally, lithium hydroxide (Tianjin Fuchen Chemical Reagent Co., Ltd., LiOH ≥ 90.0%), sodium hydroxide (Tianjin Guangfu Technology Development Co. Ltd., NaOH ≥ 98.0%), cesium hydroxide (Aladdin, 50%), ammonia solution (Tianjin Xinbote Chemical Co., Ltd., 25%~28% $NH_3 \cdot H_2O$), potassium chloride (Tianjin Fuchen Chemical Reagent Co., Ltd., KCl ≥ 99.5%), and potassium nitrate (Tianjin Xintong Fine Chemical Co., Ltd., KNO_3 ≥ 99.0%) were employed to investigate the role of K^+ and OH^- in the KFI-5.4 zeolite formation. All chemicals were utilized as received without further purification.

Materials synthesis
Preparation of OSDA (K^+)CCH
Firstly, 5.3 g of 18-crown-6 was completely dissolved in 3.5 g of deionized (DI) water to yield a colorless 18-crown-6 aqueous solution (5.7 mol·L^{-1}). Subsequently, 2.3 g of potassium hydroxide was added to the crown ether aqueous solution, resulting in an immediate yellow coloration. After stirring for 1 h, the

mixture was heated in a water bath at 80 °C for 3 h. The resulting mixture stratified, with the supernatant appearing light yellow, while the subnatant was colorless. The yellow supernatant was separated, and its chemical composition was determined to be $[(KOH)_{1.0} \cdot (18\text{-crown-}6)_{2.85} \cdot (H_2O)_{13.57}]$ [Supplementary Table 1], denoted as (K^+)CCH. The 18-crown-6/K^+ ratio of 2.85 indicates that (K^+)CCH is a mixture primarily consisting of $(KOH)_{1.0} \cdot (18\text{-crown-}6)_3$, along with minor components such as $(KOH)_{1.0} \cdot (18\text{-crown-}6)_2$ and $(KOH)_{1.0} \cdot (18\text{-crown-}6)_{1.0}$.

Synthesis of KFI-5.4 zeolite

KFI-5.4 zeolite was synthesized from an initial mixture with an optimal chemical composition of 1.4 Na_2O : 1.0 Al_2O_3 : 22.0 SiO_2 : 632 H_2O : 4.32 (K^+)CCH : 4.4 wt.% KFI-3.8 zeolite seed (based on SiO_2). In a typical synthesis of KFI-5.4 zeolite, 0.056 g of sodium aluminate and 1.2 g of prepared (K^+)CCH were added to 3.0 g of DI water. The solution was then transferred into a 25 mL Teflon beaker and stirred for 1 h. Subsequently, 0.87 g of colloidal silica was added to the solution, which was then aged at ambient temperature for 24 h under continuous stirring. After adding the KFI-3.8 seed (0.015 g), the mixture was transferred into a stainless-steel autoclave and crystallized at 150 °C for five days, 140 °C for eight days, or 120 °C for 15 days. Once the crystallization was complete, the zeolite product was filtered, washed with DI water, dried at 80 °C overnight, and calcined at 550 °C for 6 h.

NH_4/KFI-5.4 was obtained by subjecting the calcined zeolite sample to three cycles of ion exchange with a 1 mol/L ammonium chloride solution at 80 °C for 2 h. The H-KFI-5.4 sample was obtained by calcining NH_4/KFI-5.4 at 550 °C for 5 h. Na(x)-KFI-5.4 (where x = 3%, 22%, 60%, representing the Na/Al ratio multiplied by 100%) was prepared by ion-exchanging NH_4/KFI-5.4 with a sodium chloride solution, followed by calcination at 550 °C for 2 h.

Characterization

The phases of solid products were analyzed using a Rigaku D/Max 2250 X-ray diffractometer (XRD) equipped with Cu Kα radiation, scanning within a range of 2θ = 4°~40°. Morphological observations of the obtained samples were conducted using a JEOL JSM-7800F field emission scanning electron microscope (SEM). The acid property was assessed through NH_3 temperature-programmed desorption (NH_3-TPD) on a Micromeritics AutoChem II 2920. The local atomic environments were investigated using ^{13}C, ^{27}Al, and ^{29}Si solid-state magic angle spinning NMR (MAS NMR) and ^{13}C liquid NMR measurements performed on a Bruker Avance NEO system with a magnetic field intensity of 14.09 T. Bulk elemental contents were determined by inductively coupled plasma-optical emission spectrometry (ICP-OES) using a Thermo Scientific iCAP 7000 Series. Thermogravimetric analysis (TG) was carried out on a NETZSCH STA449F3 from 40 to 800 °C in air at a heating rate of 20 °C·min⁻¹.

The interactions between positive ions and 18-crown-6 were investigated via liquid-phase ultraviolet-visible (UV-Vis) absorption using a UV-Vis spectrophotometer (UV-2450) with a 2 nm slit width and a wavelength range from 200 to 700 nm. The presence of 18-crown-6 related species in (K^+)CCH was analyzed by mass spectrometry (MS) using an LCMS-9030 (SHIMADZU, Japan) equipped with an electrospray ionization source, operating in positive ionization mode. The interface voltage was set at 3.5 KV, with an interface temperature of 300 °C. Nebulizing gas (N_2) flow was 3 mL·min⁻¹; heating gas (Zero air) flow was 10 mL·min⁻¹, and drying gas (N_2) flow was 10 mL·min⁻¹. The heat block temperature was maintained at 400 °C, and the mass range analyzed ranged from 200 to 1,500 Da. The injection volume was 10 μL, and the flow rate (methanol : formic acid = 99.9:0.1) was 0.2 mL·min⁻¹.

Catalytic tests for methylamine synthesis

Typically, 0.3 g of catalyst [H-KFI-5.4, Na(3%)-KFI-5.4, Na(22%)-KFI-5.4, or Na(60%)-KFI-5.4] with 40~60 mesh size was loaded into a fixed-bed reactor. The catalyst was pretreated in flowing nitrogen at 380 °C for 1 h and then cooled to the desired reaction temperature of 300 or 350 °C. Subsequently, pure NH_3 gas was introduced into the reactor followed by MeOH carried into the reactor by N_2 (38.0 mL·min^{-1}), which had passed through a saturator containing liquid MeOH. The weight hourly space velocity of MeOH ($WHSV_{MeOH}$) was maintained at 0.813 h^{-1}, and the molar ratio of NH_3 to MeOH was kept at 2/1. The partial pressures of MeOH, NH_3, and N_2 were 6.7, 13.4, and 81.2 kPa, respectively.

For comparison, the activity of the H-KFI-5.4 catalyst was also measured at a reaction temperature of 400 °C under conditions of 4.3 h^{-1} $WHSV_{MeOH}$ and 1.0 NH_3/MeOH, conditions very similar to those reported for H-rho and H-PST-29[9]. The gaseous products were analyzed online using an Agilent 7890 gas chromatograph equipped with a flame ionization detector and a CP-Volamine capillary column. The selectivity and yield were calculated based on carbon-based products.

RESULTS AND DISCUSSION

Textural property of KFI-5.4 zeolite

The experimental XRD pattern of KFI-5.4 zeolite (synthesis condition: 150 °C, 5 days) is depicted in Figure 1A, demonstrating a match to the simulated pattern. Figure 1B presents the SEM image of **KFI** crystals, revealing irregularly shaped aggregates composed of intergrown micrometer cubic-like crystals, consistent with prior reports on **KFI** crystals[27]. These findings affirm the successful synthesis of pure and highly crystalline KFI zeolite.

The TG curve of KFI-5.4 zeolite is displayed in Figure 1C. The weight loss of 8.66 wt.% observed at 40~250 °C corresponds to the desorption of physically adsorbed water, while the 4.83 wt.% weight loss at 250~800 °C is attributed to the decomposition of the OSDA[28,29], indicating the presence of OSDA in KFI-5.4 zeolite.

Furthermore, the ^{13}C MAS NMR spectrum of KFI-5.4 zeolite [Figure 1D] reveals a signal at 69.2 ppm, attributed to the oxygen-substituted methylene carbon[30,31], consistent with the liquid ^{13}C NMR spectrum of (K^+)CCH. This confirms that the as-prepared K^+ and 18-crown-6 complex is occluded in the KFI-5.4 zeolite as an OSDA.

The ^{27}Al MAS NMR spectrum [Figure 1E] exhibits a resonance peak at 59 ppm assigned to tetrahedral aluminum, indicating the absence of extra-framework aluminum species in KFI-5.4 zeolite[32,33]. Additionally, the ^{29}Si MAS NMR spectrum [Figure 1F] displays three major signals at around -110, -105, and -99 ppm, assigned to Si(0Al), Si(1Al), and Si(2Al), respectively[19,34]. Based on the deconvolution results of Si(nAl) species, the Si/Al ratio of KFI-5.4 zeolite is calculated to be 5.4, closely matching the value of 5.8 determined via ICP-OES analyses. These comprehensive analyses confirm the successful synthesis of zeolite **KFI** with a higher Si/Al ratio than previously reported.

Influence of the synthetic parameters on the KFI-5.4 zeolite crystallization

Crystallization temperature

The crystallization temperature is widely recognized as a critical factor influencing both the thermodynamics and kinetics of zeolite crystallization[35-37]. Hydrothermal treatment at different crystallization temperatures (100, 120, 140, and 160 °C) yielded varying products from the initial mixtures optimized for KFI-5.4 zeolite [Figure 2A]. At 100 °C, an amorphous product was obtained, while a mixture
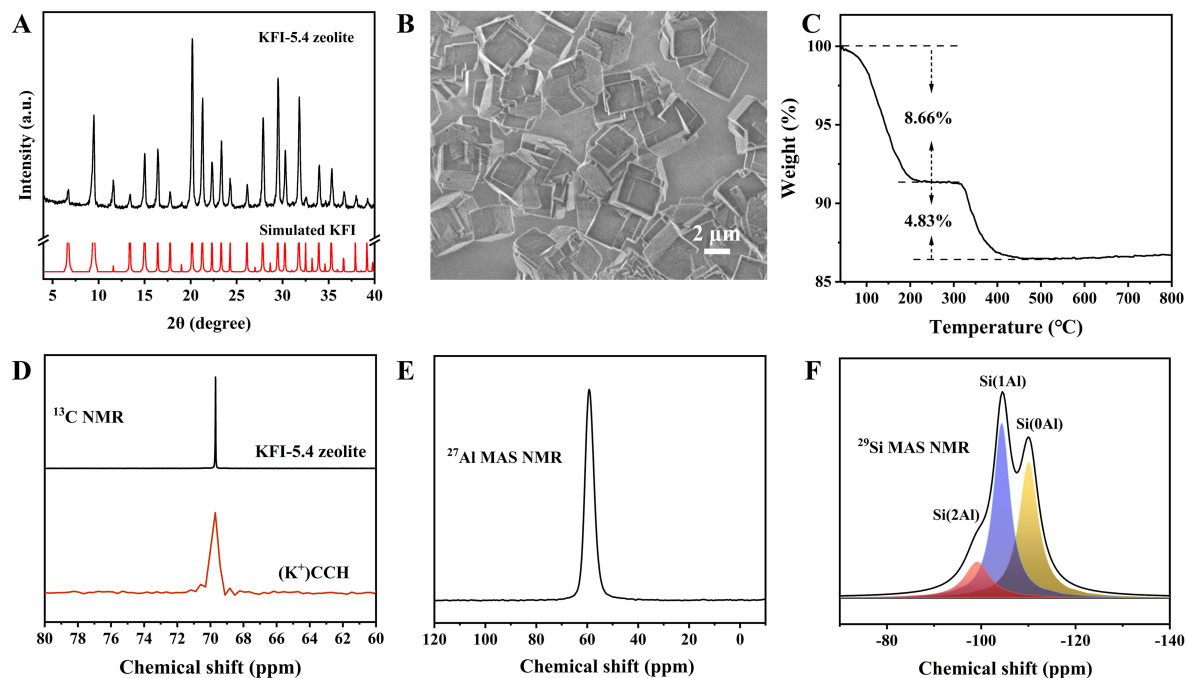
Figure 1. (A) Simulated XRD pattern (bottom) of **KFI** and experimental XRD pattern (top); (B) SEM image; and (C) TG curve of KFI-5.4 zeolite (synthesis condition: 150 °C, 5 days); (D) ^{13}C liquid NMR spectrum (bottom) of (K^{+})CCH and ^{13}C solid-state MAS NMR spectrum (top) of KFI-5.4 zeolite; (E) ^{27}Al and (F) ^{29}Si solid-state MAS NMR spectra of KFI-5.4 zeolite. XRD: X-ray diffractometer; SEM: scanning electron microscope; TG: thermogravimetric analysis; NMR: nuclear magnetic resonance; MAS: magic angle spinning.
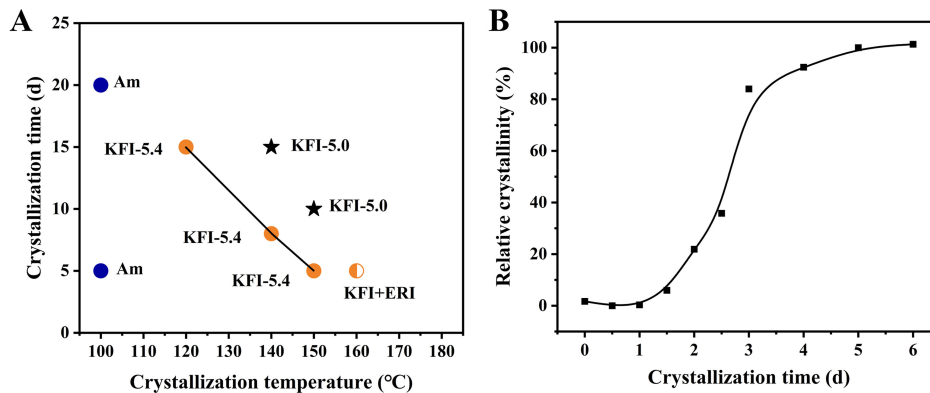

Figure 2. (A) Influence of crystallization temperature and time on the formation of KFI-5.4 zeolite. The phases of KFI-5.4 zeolite marked with circles were obtained in this work, while the phases of the KFI-5.0 zeolites (framework Si/Al = 5.0) marked with stars were reported by the reference[21]. "Am" represents an amorphous material; (B) Crystallization curve of KFI-5.4 zeolite at 150 °C.

of **KFI** and **ERI** was acquired at 160 °C. Thus, the suitable crystallization temperature range for KFI-5.4 zeolite lies between 120~150 °C, albeit with differing crystallization periods. Pure and highly crystalline KFI-5.4 zeolite was formed at 140 or 120 °C with crystallization times of 8 and 15 days, respectively (Experimental XRD patterns are shown in Supplementary Figure 1). However, a crystallization time of 5 days sufficed at 150 °C. The crystallization curve [Figure 2B] and SEM images [Supplementary Figure 2] elucidate the detailed crystallization process. The initial mixture (0 day) exhibited extremely low crystallinity due to the presence of a few KFI-3.8 seeds and a significant amount of amorphous aluminosilicate species.

As the crystallization time increased from 0 to 1 day, the crystallinity decreased, indicating the dissolution of KFI-3.8 seeds. Extending the crystallization time to 1.5~4 days resulted in a gradual increase in product crystallinity. Ultimately, pure and fully crystalline KFI-5.4 zeolite was obtained after 5 days of crystallization, representing a twofold reduction in crystallization time compared to other high-silica **KFI** zeolites (framework Si/Al = 5.0, denoted as KFI-5.0 and marked with a star in Figure 2A)[21].

Chemical compositions of the initial mixture

The influence of the SiO_2/Al_2O_3, H_2O/Al_2O_3, and OH^-/Al_2O_3 ratios of the initial mixture was further explored at a crystallization temperature of 150 °C. The summarized results are presented in Figure 3, with corresponding X-ray diffraction (XRD) patterns of the products shown in Supplementary Figures 3-5. Notably, the presence of KFI-3.8 zeolite seed was found to be crucial for the crystallization of KFI-5.4 [Supplementary Figure 6], suggesting that the KFI-3.8 zeolite seed provides the necessary nucleation site for the target **KFI** framework[38-40].

Maintaining the H_2O/Al_2O_3 ratio at 632 and the OH^-/Al_2O_3 ratio at 4.32 (represented by horizontal lines in Figure 3A and B), pure **KFI** zeolite was obtained when the SiO_2/Al_2O_3 ratio of the initial mixture was 20.6 or 19.6. However, the Si/Al ratio of the resultant **KFI** zeolite decreased to 5.1 and 4.5, respectively. Conversely, when the SiO_2/Al_2O_3 ratio increased to 23.4, an undesirable amorphous phase formed. The optimal product, pure **KFI** zeolite with the highest framework Si/Al ratio of 5.4, was attained at a SiO_2/Al_2O_3 ratio of 22.0.

Under these optimal conditions, the influence of the H_2O/Al_2O_3 ratio of the initial mixture, ranging from 211 to 1,054, was investigated while maintaining the SiO_2/Al_2O_3 ratio at 22.0 and the OH^-/Al_2O_3 ratio at 4.32. As depicted by the vertical line in Figure 3A and the XRD patterns in Supplementary Figure 4, the crystallinities of the **KFI** zeolite products significantly decreased when the H_2O/Al_2O_3 ratio fell below 421 or exceeded 841, forming an amorphous phase. Pure KFI-5.4 zeolite with high crystallinity was obtained at an H_2O/Al_2O_3 ratio of 632.

Furthermore, the influence of the OH^-/Al_2O_3 ratio of the initial mixture, varying from 2.88 to 5.76, on the crystallization of KFI-5.4 was explored while maintaining the SiO_2/Al_2O_3 ratio at 22.0 and the H_2O/Al_2O_3 ratio at 632, with OH^- introduced by $(K^+)CCH$. As illustrated by the vertical line in Figure 3B, an amorphous product was obtained at an OH^-/Al_2O_3 ratio of 2.88. At an OH^-/Al_2O_3 ratio of 3.60, **KFI** zeolite, along with an amorphous phase, was obtained, while a co-crystallized product of **KFI** and **ERI** zeolite formed at OH^-/Al_2O_3 ratios of 5.04 or 5.76. Highly crystalline KFI-5.4 zeolite was formed at an OH^-/Al_2O_3 ratio of 4.32.

New OSDA $(K^+)CCH$

In this study, the addition of KOH to the 18-crown-6 aqueous solution led to the observation of stratification phenomenon and color change, possibly due to the interaction between K^+ and crown ether. This interaction was investigated through liquid-phase UV-Vis adsorption. The UV-Vis adsorption spectra of $(K^+)CCH$ diluted with various fractions of DI water [Figure 4 and Supplementary Figure 7] revealed a distinctive band at 352 nm, attributed to the charge transfer between K^+ and crown ether[41]. Notably, this band was absent in the UV-Vis spectra of pure 18-crown-6 or KOH aqueous solutions [Supplementary Figures 8 and 9], indicating the formation of a strong interaction between K^+ and 18-crown-6 in the (K^+) CCH complex. Furthermore, the discrepancy in XRD patterns between pure 18-crown-6 and $(K^+)CCH$ powders obtained from vacuum freeze-drying further corroborated the existence of a strong interaction between K^+ and 18-crown-6 [Supplementary Figure 10].
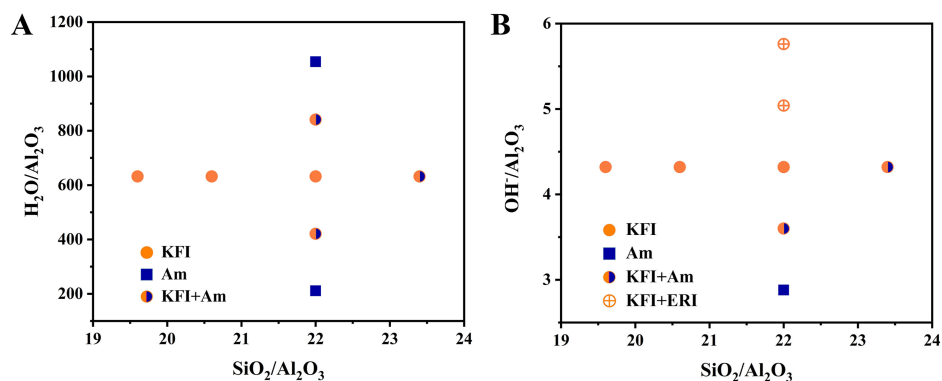
Figure 3. Influence of (A) SiO_2/Al_2O_3 and H_2O/Al_2O_3, and (B) SiO_2/Al_2O_3 and OH^-/Al_2O_3 ratios in the initial mixtures on the products crystallized. The initial mixtures compositions are as follows: 1.4 Na_2O : 1.0 Al_2O_3 : 19.6~23.4 SiO_2 : 211~1,054 H_2O : 2.88~5.76 OH^-, where OH^- was introduced by OSDA $(K^+)CCH$. OSDA: Organic structure-directing agent.
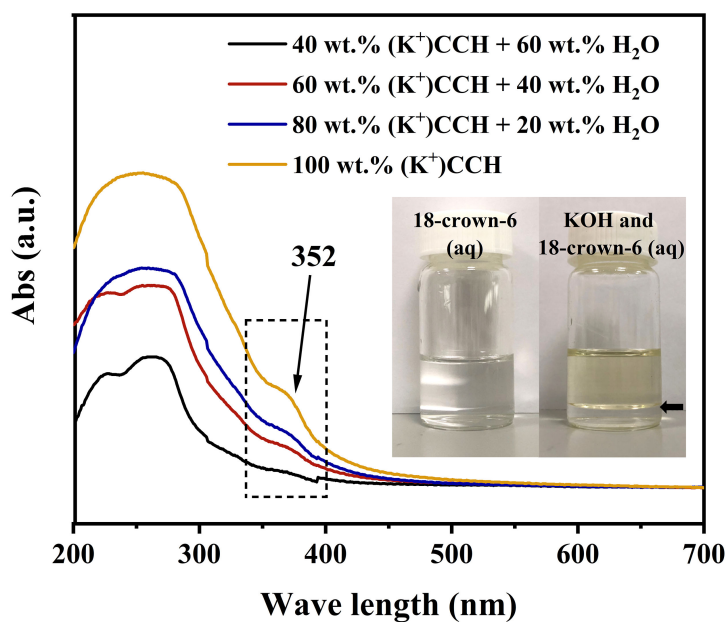

Figure 4. UV-Vis adsorption spectra of $(K^+)CCH$ diluted with different fractions of DI water, and the inserted photographs for the 18-crown-6 aqueous solution (5.7 mol·L^{-1}) and the mixture of 18-crown-6 aqueous solution (5.7 mol·L^{-1}) with KOH. UV-Vis: Ultraviolet-visible.

To gain further insights into the structure of $(K^+)CCH$, we conducted MS analysis on the 18-crown-6 related species present in $(K^+)CCH$. A peak at m/z 795.2272 was observed in the mass spectrum of $(K^+)CCH$ [Supplementary Figure 11], corresponding to $[3(18\text{-crown-6})+3H]^+$, indicating the presence of three 18-crown-6 molecules within $(K^+)CCH$. This suggests a highly stable complex formation. Bulk OSDAs with lower charge densities have been identified as favorable for synthesizing high-silica zeolites[22,42]. In the typical complex between K^+ and 18-crown-6, the 18-crown-6/K^+ ratio is usually 1. However, in $(K^+)CCH$, this ratio increases to 2.85, indicating a significantly lower charge density.

To elucidate the role of (K⁺)CCH in directing the formation of KFI-5.4 zeolite, we replaced the as-prepared (K⁺)CCH with equivalent chemicals of H_2O, KOH, and 18-crown-6 under identical crystallization conditions. Only **KFI** zeolite with low crystallinity was obtained [Supplementary Figure 12], suggesting that the stable structure of (K⁺)CCH plays a critical role in the formation of KFI-5.4 zeolite.

Control experiments were conducted to investigate the roles of K⁺ and OH⁻ in the formation of KFI-5.4 zeolite, and the results are summarized in Figure 5. Four types of hydroxides, namely LiOH, NaOH, CsOH, and $NH_3·H_2O$ (NH_4OH), were added to a colorless 18-crown-6 aqueous solution (5.7 mol·L⁻¹), with the mole of each hydroxide equal to that of KOH, respectively. After stirring in the water bath for the same duration as that of KOH, different mixtures were obtained. Photographs of these mixtures are provided in the inset of Figure 6 (i.e., 18-crown-6 aqueous solution mixed with NaOH, CsOH, or $NH_3·H_2O$) and Supplementary Figure 13A (18-crown-6 aqueous solution mixed with LiOH). Notably, LiOH could not be completely dissolved in the 18-crown-6 aqueous solution. Upon addition of $NH_3·H_2O$ to the 18-crown-6 aqueous solution, a colorless mixture was formed. However, when NaOH or CsOH was added to the 18-crown-6 aqueous solution, a stratified mixture with a yellow supernatant was obtained, similar to the mixture of KOH and 18-crown-6 aqueous solution. These observations suggest that Na⁺ and Cs⁺ can interact with 18-crown-6, while the interaction between NH_4^+ and 18-crown-6 is uncertain.

The interactions between the positive ions and 18-crown-6 were further examined through liquid-phase UV-Vis adsorption. In the UV-Vis adsorption spectra [Figure 6 and Supplementary Figure 14] of the yellow supernatant of the Na⁺ with 18-crown-6 mixture [designated as (Na⁺)CCH], a band at 315 nm is observed, indicative of ligand-to-metal charge transfer[43,44], suggesting that Na⁺ is bound to 18-crown-6. Similarly, a band at 317 nm is observed in the UV-Vis adsorption spectra [Figure 6 and Supplementary Figure 15] of the yellow supernatant of the Cs⁺ with 18-crown-6 mixture [designated as (Cs⁺)CCH], indicating that Cs⁺ is also bound to 18-crown-6[45]. In contrast, the mixture of $NH_3·H_2O$ and 18-crown-6 exhibits a band similar to that of the 18-crown-6 aqueous solution (228 *vs.* 225 nm) in the UV-Vis adsorption spectra [Figure 6 and Supplementary Figure 16], suggesting no interaction between NH_4^+ and 18-crown-6 in the $NH_3·H_2O$ and 18-crown-6 mixture.

Subsequently, the yellow supernatant of (Na⁺)CCH or (Cs⁺)CCH, instead of (K⁺)CCH, was added to the initial mixture for the crystallization of KFI-5.4. After heating at 150 °C for 5 days, no **KFI** zeolite was obtained [Figure 5], indicating that only the 18-crown-6 complex of K⁺ serves as the structure-directing agent for KFI-5.4 zeolite, even though other metal ions can also form complexes with 18-crown-6.

Furthermore, the role of OH⁻ was investigated using alternative potassium sources instead of KOH, and the results are presented in Figure 5. In this experiment, KNO_3 or KCl, equimolar to KOH, was added to the 18-crown-6 aqueous solution (5.7 mol·L⁻¹) and then heated in a water bath. However, the solid could not be completely dissolved (Photographs are shown in Supplementary Figure 13B and C, respectively). This observation demonstrates that OH⁻ facilitates the dissolution of K⁺ in the 18-crown-6 aqueous solution, thereby forming a complex of K⁺ and 18-crown-6.

Catalytic performance

The catalytic performances of H-KFI-5.4 and other reported small-pore zeolites are summarized in Table 1. Under the conditions of 0.813 h⁻¹ WHSV$_{MeOH}$ and NH_3/MeOH ratio of 2, it is observed that the MMA plus DMA selectivity increases to 78.9% from 76.9%, and the MeOH conversion significantly rises to 95.2% from 49.9% with the reaction temperature raised from 300 to 350 °C, thereby greatly improving the yield for MMA plus DMA from 38.4% to 75.1%. Although H-KFI-3.2 exhibits a higher selectivity of 86.2% for MMA

Table 1. Comparison of the catalytic performances in the shape-selective synthesis of MAs over as-synthesized high-silica KFI-5.4 zeolite in this work and previously reported small-pore zeolites

| Catalyst | Si/Al | T (°C)[a] | MeOH conversion (%) | Selectivity (%) | | | | (MMA + DMA) yield (%)[c] | Ref. |
				MMA	DMA	TMA	(MMA + DMA)[b]		
H-KFI-5.4	5.4	300	49.9	35.9	41.0	10.2	76.9	38.4	This work
		350	95.2	24.1	54.8	17.1	78.9	75.1	
		400	49.6	36.1	33.6	15.7	69.7	34.6	
Na(3%)-KFI-5.4	5.4	350	97.0	22.7	54.4	19.7	77.1	74.8	
Na(22%)-KFI-5.4	5.4	350	95.0	26.0	56.4	16.6	82.4	78.3	
Na(60%)-KFI-5.4	5.4	350	72.1	35.6	51.6	11.4	87.2	62.9	
H-KFI-3.2	3.2	350	63.4	33.7	52.5	5.1	86.2	54.7	[8]
SAPO-34[d]	-	350	51.1	34.2	48.9	10.4	83.1	42.5	[11]
		380	82.0	26.8	54.7	14.5	81.5	66.8	
DNL-6[e]	-	260	49.7	42.1	36.2	4.6	78.3	38.9	[10]
		300	88.3	26.1	45.9	12.5	72.0	63.6	
H-rho	3.9	400	~35.0	-	-	-	-	~31.0	[9]
H-PST-29	4.5	400	~48.0	-	-	-	-	~39.0	

[a]Activities at 260, 300, 350, and 380 °C recorded under the condition of 0.813 h^{-1} WHSV$_{MeOH}$ and 2.0 NH$_3$/MeOH, and at 400 °C recorded under the condition of 4.3 h^{-1} WHSV$_{MeOH}$ and 1.0 NH$_3$/MeOH after 600 min on stream; [b]MMA plus DMA selectivity in all carbon-based products; [c]MMA plus DMA yield = MeOH conversion × MMA plus DMA selectivity in all carbon-based products; [d]Chemical composition: Si$_{0.189}$Al$_{0.463}$P$_{0.348}$, framework type: **CHA**; [e]Chemical composition: Si$_{0.364}$Al$_{0.414}$P$_{0.222}$O$_2$, framework type: **RHO**. MAs: Methylamines; MMA: monomethylamine; DMA: dimethylamine; TMA: trimethylamine.
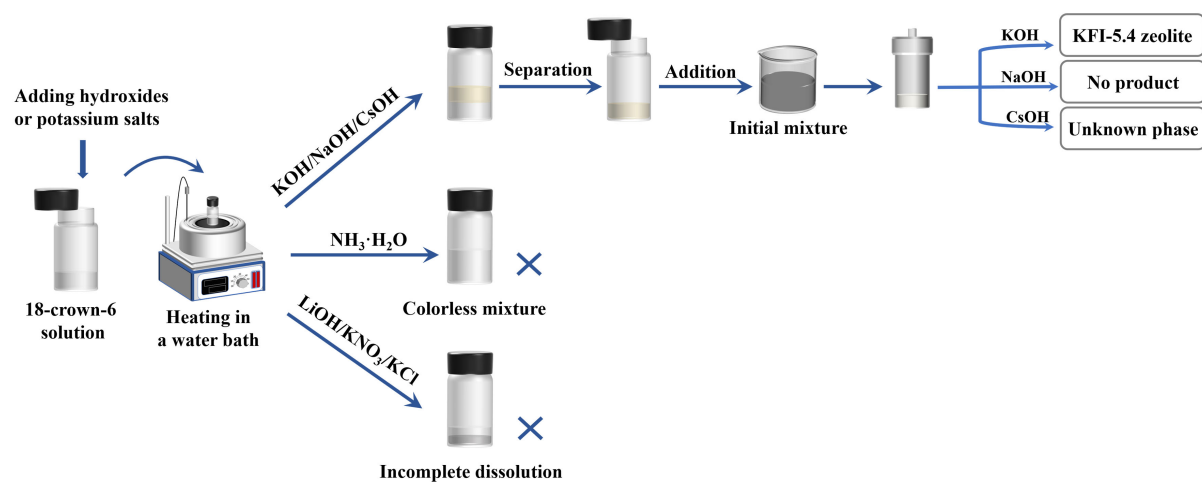
Figure 5. Control experiments investigating the role of K$^+$ and OH$^-$ in the formation of KFI-5.4 zeolite.

plus DMA, the lower MeOH conversion of 63.4% results in a lower MMA plus DMA yield of 54.7%[8]. Previous studies have indicated that increasing the Si/Al ratio of zeolite could enhance the strength of the Brønsted acid sites, thus improving the MeOH conversion and MMA plus DMA yield[23]. Based on this observation, it is reasonable to conclude that the MeOH conversion and MMA plus DMA yield of H-KFI-5.4 are higher than those of H-KFI-3.2. Furthermore, H-KFI-5.4 exhibits a superior MMA plus DMA yield compared to SAPO-34[11]. Although the MMA plus DMA yield of DNL-6 at 300 °C (63.6%) is much better than that at 260 °C (38.9%), it remains lower than that of H-KFI-5.4 at 350 °C[10]. Under similar conditions, i.e., 400 °C, 4.3 h^{-1} WHSV$_{MeOH}$, and 1.0 NH$_3$/MeOH, the H-KFI-5.4, H-rho, and H-PST-29 exhibit comparable MMA plus DMA yields Supplementary Figure 18[9]. These results indicate that H-KFI-5.4
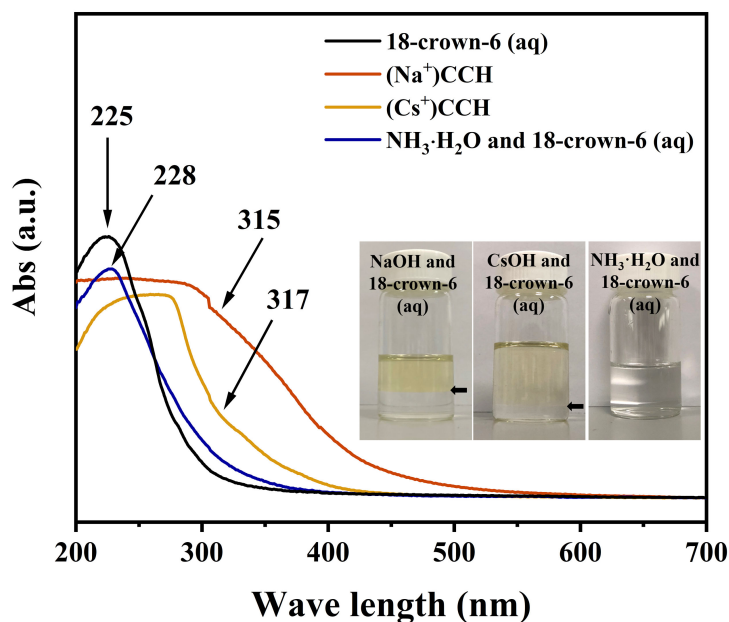
Figure 6. UV-Vis adsorption spectra of $(Na^+)CCH$, $(Cs^+)CCH$, $NH_3 \cdot H_2O$ and 18-crown-6 (aq) mixture, and 18-crown-6 aqueous solution (5.7 mol·L^{-1}), and the inserted photographs for the mixtures of 18-crown-6 (5.7 mol·L^{-1}) aqueous solutions with NaOH, CsOH, and $NH_3 \cdot H_2O$, respectively. UV-Vis: Ultraviolet-visible.

possesses the top level of catalytic performance among the small-pore zeolites reported up to date, demonstrating that KFI-5.4 is a promising solid catalyst for the shape-selective synthesis of MAs.

We further prepared Na(3%)-KFI-5.4, Na(22%)-KFI-5.4, and Na(60%)-KFI-5.4 catalysts and investigated the influence of Na$^+$ loading on MeOH conversion and product formation. As shown in Figure 7A-C and Supplementary Figure 19 and summarized in Table 1, the extremely low Na$^+$ loading (i.e., Na/Al ratio × 100% = 3%) has no significant influence on the MeOH conversion and the selectivity/yield of MMA plus DMA. When the Na$^+$ loading increases to 22%, MeOH conversion remains almost unchanged, while the selectivity of MMA and DMA significantly rises, thereby enhancing the yield of MMA plus DMA. However, further increasing the Na$^+$ loading to 60% results in an increase in MMA plus DMA selectivity but a significant reduction in MeOH conversion, ultimately reducing the yield of MMA plus DMA.

It is worth noting that DME is not formed for Na(22%)-KFI-5.4 and Na(60%)-KFI-5.4 catalysts, and the DME selectivity reduction is closely aligned with the increase in MA selectivity for Na(22%)-KFI-5.4 or Na(60%)-KFI-5.4 [Figure 7D]. This observation is consistent with previously reported findings indicating that Na$^+$ can suppress the DME formation[25,46]. Therefore, it is inferred that the presence of Na$^+$ alters the reaction pathway, thereby inhibiting the DME formation while promoting the generation of MAs. This phenomenon contributes to improving the yield and/or selectivity of the catalyst, explaining the similarity between the decrease in DME and the enhancement of MA selectivity in reactions catalyzed by Na(22%)-KFI-5.4 and Na(60%)-KFI-5.4. However, an excessive amount of Na$^+$ in Na(60%)-KFI-5.4 will occupy a significant portion of the acid sites and restrict the accessibility of the KFI framework, resulting in a substantial reduction in MeOH conversion and, consequently, decreasing the yield of MMA plus DMA.
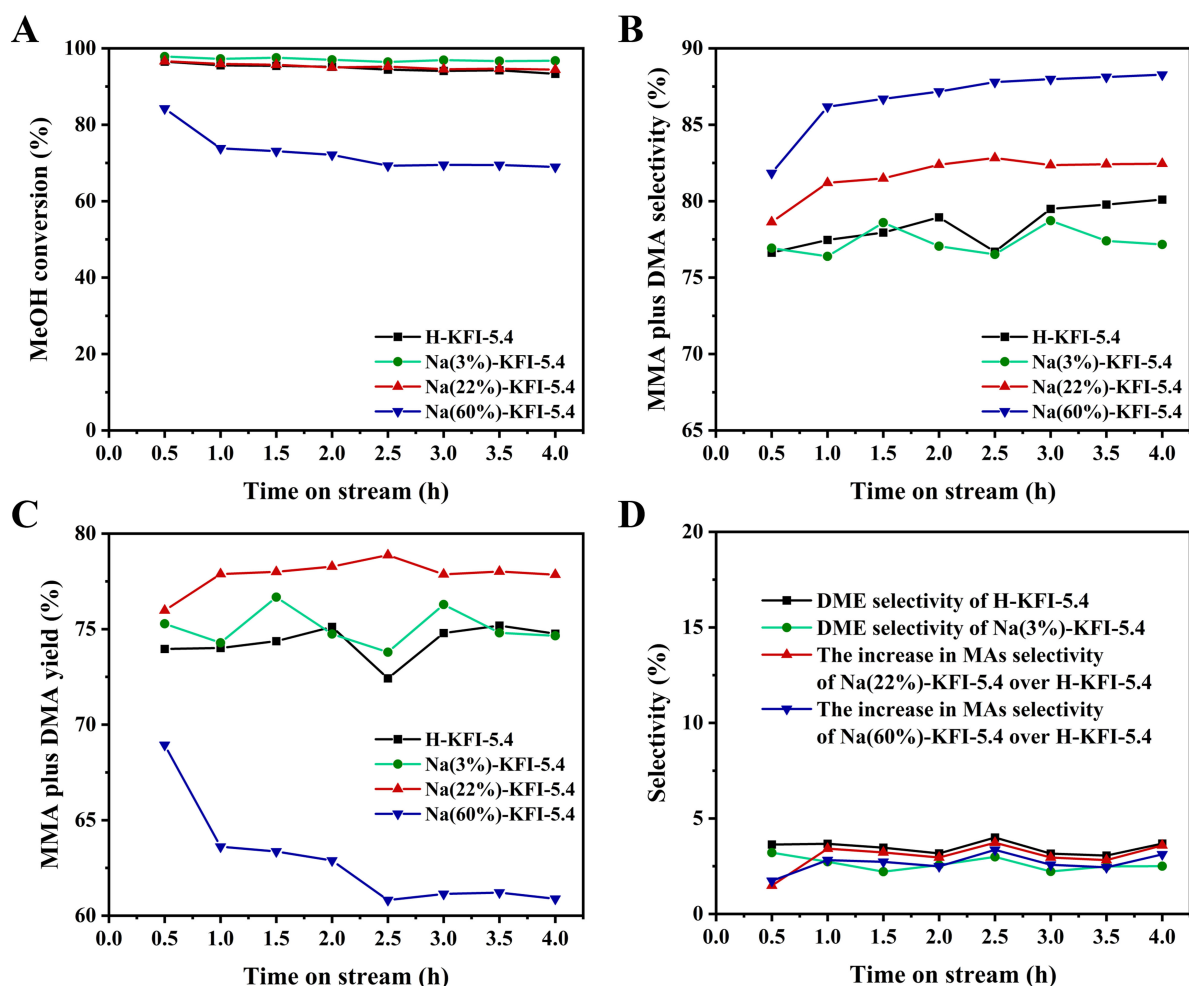
Figure 7. (A) MeOH conversion; (B) MMA plus DMA selectivity; and (C) MMA plus DMA yield over H-KFI-5.4, Na(3%)-KFI-5.4, Na(22%)-KFI-5.4, and Na(60%)-KFI-5.4 catalysts; (D) DME selectivity of H-KFI-5.4 and Na(3%)-KFI-5.4, and the increase in MA selectivity of Na(22%)-KFI-5.4 or Na(60%)-KFI-5.4 over H-KFI-5.4 in MA synthesis at 350 °C, 0.813 h^{-1} WHSV$_{MeOH}$, and 2.0 NH$_3$/MeOH. MMA: Monomethylamine; DMA: dimethylamine; DME: dimethyl ether; MA: methylamine; WHSV: weight hourly space velocity.

CONCLUSIONS

The low-silica H-KFI-3.2 exhibited superior MMA plus DMA selectivity but lower MeOH conversion (63.4%), resulting in a reduced MMA plus DMA yield (54.7%) in the shape-selective synthesis of MAs, thus limiting its potential application in MA synthesis. To address this limitation, **KFI** zeolite with a high framework Si/Al ratio of 5.4 was rapidly synthesized using a newly developed OSDA of 18-crown-6/K$^+$ complex [(K$^+$)CCH]. The stable structure of the (K$^+$)CCH complex proved crucial for forming KFI-5.4 zeolite. The high-silica **KFI** zeolite obtained in this study exhibited top-level catalytic performance, with high MeOH conversion (95.2%) and MMA plus DMA yield (75.1%) among small-pore zeolites reported to date. This highlights KFI-5.4 as a promising solid catalyst for the shape-selective synthesis of MAs. Moreover, we discovered that a Na$^+$ loading of 22% further enhanced the yield and selectivity of MMA plus DMA. This research presents a high-performance catalyst for MMA and DMA synthesis and offers an effective zeolite modification method to improve the yield and selectivity of MMA plus DMA in MA synthesis.

DECLARATIONS

Authors' contributions

Conceptualization, investigation, methodology, data curation, formal analysis, writing - original draft: Wu R
Conceptualization, methodology, formal analysis, writing - review and editing: Han J
Data curation: Li J
Data curation, writing - review and editing: Li L
Investigation, formal analysis: Liu S
Conceptualization, funding acquisition, writing - review and editing: Tian P
Conceptualization, funding acquisition, resources, supervision, project administration, writing - review and editing: Yan W

Availability of data and materials

Experimental details on synthesis, characterization, and catalysis are available in the Supplementary Materials, and the data supporting the findings of this study are available within its supplementary materials.

Financial support and sponsorship

Conflicts of interest

All authors declared that there are no conflicts of interest.

Ethical approval and consent to participate

Not applicable.

Consent for publication

Not applicable.

Copyright

REFERENCES

1. Kumar R, Karmilowicz MJ, Burke D, et al. Biocatalytic reductive amination from discovery to commercial manufacturing applied to abrocitinib JAK1 inhibitor. *Nat Catal* 2021;4:775-82. DOI
2. Liu J, Guo C, Zhang Z, et al. Synthesis of dimethylformamide from CO_2, H_2 and dimethylamine over Cu/ZnO. *Chem Commun* 2010;46:5770-2. DOI PubMed
3. Lammens TM, Franssen MCR, Scott EL, Sanders JPM. Synthesis of biobased N-methylpyrrolidone by one-pot cyclization and methylation of γ-aminobutyric acid. *Green Chem* 2010;12:1430-6. DOI
4. Corbin DR, Schwarz S, Sonnichsen GC. Methylamines synthesis: a review. *Catal Today* 1997;37:71-102. DOI
5. Bosch M, Röttger R, Eberhardt J, et al. Shaped body comprising an aluminosilicate and aluminium oxide and process for the continuous preparation of methylamines. Available from: https://ppubs.uspto.gov/dirsearch-public/print/downloadPdf/7754921. [Last accessed on 22 Apr 2024].
6. Jeon H, Shin C, Jung HJ, Hong SB. Catalytic evaluation of small-pore molecular sieves with different framework topologies for the synthesis of methylamines. *Appl Catal A Gen* 2006;305:70-8. DOI
7. Ashina Y, Fujita T, Fukatsu M, Niwa K, Yagi J. Manufacture of dimethylamine using zeolite catalyst. *Stud Surf Sci Catal* 1986;28:779-86. DOI
8. Wu R, Han J, Wang Y, et al. Exclusive SAPO-seeded synthesis of ZK-5 zeolite for selective synthesis of methylamines. *Inorg Chem Front* 2022;9:5766-73. DOI
9. Lee H, Lee K, Shin J, Hong SB. A comparative study of methylamines synthesis over zeolites H-rho and H-PST-29. *Microporous*

Mesoporous Mater 2020;300:110150. DOI

10.   Wu P, Yang M, Zhang W, et al. Silicoaluminophosphate molecular sieve DNL-6: synthesis with a novel template, *N,N′*-dimethylethylenediamine, and its catalytic application. *Chin J Catal* 2018;39:1511-9. DOI

11.   Qiao Y, Wu P, Xiang X, et al. SAPO-34 synthesized with n -butylamine as a template and its catalytic application in the methanol amination reaction. *Chin J Catal* 2017;38:574-82. DOI

12.   van Well WJM, Jänchen J, de Haan JW, van Santen RA. Adsorption of linear alkanes in the α-cages and γ-cages of H-ZK-5 and K-ZK-5. *J Phys Chem B* 1999;103:1841-53. DOI

13.   Barrer RM. Synthesis of a zeolitic mineral with chabazite-like sorptive properties. *J Chem Soc* 1948:127-32. DOI PubMed

14.   United States Patent Office. 1966. Synthetic zeolite and method for preparing the same. George T. Kerr, Trenton, N.J., assignor to Socony Mobil Oil Company, Inc., a corporation of New York. No Drawing. Filed Jan. 4, 1965, Ser. No. 423,346. 14 Claims. (Ci.260 -242). Available from: https://ppubs.uspto.gov/dirsearch-public/print/downloadPdf/3247195. [Last accessed on 22 Apr 2024].

15.   Chatelain T, Patarin J, Farré R, Pétigny O, Schulz P. Synthesis and characterization of 18-crown-6 ether-containing KFI-type zeolite. *Zeolites* 1996;17:328-33. DOI

16.   Remy T, Peter SA, Van Tendeloo L, et al. Adsorption and separation of CO_2 on KFI zeolites: effect of cation type and Si/Al ratio on equilibrium and kinetic properties. *Langmuir* 2013;29:4998-5012. DOI

17.   Remy T, Gobechiya E, Danaci D, et al. Biogas upgrading through kinetic separation of carbon dioxide and methane over Rb- and Cs-ZK-5 zeolites. *RSC Adv* 2014;4:62511-24. DOI

18.   Ji Y, Birmingham J, Deimund MA, Brand SK, Davis ME. Steam-dealuminated, OSDA-free RHO and KFI-type zeolites as catalysts for the methanol-to-olefins reaction. *Microporous Mesoporous Mater* 2016;232:126-37. DOI

19.   Kim J, Cho SJ, Kim DH. Facile synthesis of KFI-type zeolite and its application to selective catalytic reduction of NO*x* with NH_3. *ACS Catal* 2017;7:6070-81. DOI

20.   Lozinska MM, Bruce EL, Mattock J, et al. Understanding the anion-templated, OSDA-free, interzeolite conversion synthesis of high silica zeolite ZK-5. *Chemistry* 2022;28:e202201689. DOI PubMed PMC

21.   Han S, Tang X, Wang L, et al. Potassium-directed sustainable synthesis of new high silica small-pore zeolite with KFI structure (ZJM-7) as an efficient catalyst for NH_3-SCR reaction. *Appl Catal B Environ* 2021;281:119480. DOI

22.   Li J, Gao M, Yan W, Yu J. Regulation of the Si/Al ratios and Al distributions of zeolites and their impact on properties. *Chem Sci* 2023;14:1935-59. DOI PubMed PMC

23.   Tijsebaert B, Yilmaz B, Müller U, et al. Shape-selective synthesis of methylamines over the RRO zeolite Al-RUB-41. *J Catal* 2011;278:246-52. DOI

24.   Veefkind VA, Gründling C, Lercher JA. Steric aspects in methylamine and dimethylether synthesis over acidic mordenites. *J Mol Catal A Chem* 1998;134:111-9. DOI

25.   Maeda N, Meemken F, Hungerbühler K, Baiker A. Selectivity-controlling factors in catalytic methanol amination studied by isotopically modulated excitation IR spectroscopy. *ACS Catal* 2013;3:219-23. DOI

26.   Zhang YZ, Xu ZL, Wang J, Ke YY. Studies on the nature of catalysts for the selective synthesis of methylamine. *Stud Surf Sci Catal* 1994;84:1927-33. DOI

27.   Kamimura Y, Endo A. Seed-assisted, organic structure-directing agent-free synthesis of KFI-type zeolite with enhanced micropore volume and CO_2 adsorption capacity. *Adsorption* 2019;25:1099-113. DOI

28.   Yang Y, Meng X, Zhu L, et al. Rapid synthesis of Si-rich SSZ-13 zeolite under fluoride-free conditions. *Inorg Chem* 2022;61:21115-22. DOI

29.   Mi Z, Li J, Lu T, et al. Reducing the dosage of the organic structure-directing agent in the crystallization of pure silica zeolite MFI (silicalite-1) for volatile organic compounds (VOCs) adsorption. *Inorg Chem Front* 2021;8:3354-62. DOI

30.   Roslund MU, Tähtinen P, Niemitz M, Sjöholm R. Complete assignments of the ^{1}H and ^{13}C chemical shifts and $J_{H,H}$ coupling constants in NMR spectra of D-glucopyranose and all D-glucopyranosyl-D-glucopyranosides. *Carbohydr Res* 2008;343:101-12. DOI PubMed

31.   Glinel K, Sauvage JP, Oulyadi H, Huguet J. Determination of substituents distribution in carboxymethylpullulans by NMR spectroscopy. *Carbohydr Res* 2000;328:343-54. DOI PubMed

32.   Liang J, Fu W, Liu C, et al. Synthesis of FER zeolite using 4-(aminomethyl)pyridine as structure-directing agent. *Chem Res Chin Univ* 2022;38:243-9. DOI

33.   Ye Z, Kong L, Zhao Y, et al. Alkalinity-controlled zeolite nucleation and growth: ultrafast synthesis of total-morphology zeolite L mesocrystals and adsorption evaluation. *Chem Synth* 2022;2:20. DOI

34.   Zhang Y, Dai W, Wu G, Guan N, Li L. Catalytic hydration of aromatic alkynes to ketones over H-MFI zeolites. *Chem Res Chin Univ* 2022;38:173-80. DOI

35.   Bian C, Zhang C, Pan S, et al. Generalized high-temperature synthesis of zeolite catalysts with unpredictably high space-time yields (STYs). *J Mater Chem A* 2017;5:2613-8. DOI

36.   Mi Z, Lu T, Zhang J, Xu R, Yan W. Synthesis of pure silica zeolites. *Chem Res Chin Univ* 2022;38:9-17. DOI

37.   Tai W, Dai W, Wu G, Li L. A simple strategy for synthesis of *b*-axis-oriented MFI zeolite macro-nanosheets. *Chem Synth* 2023;3:38. DOI

38.   Kamimura Y, Tanahashi S, Itabashi K, et al. Crystallization behavior of zeolite Beta in OSDA-free, seed-assisted synthesis. *J Phys Chem C* 2011;115:744-50. DOI

39.   Zhang H, Wang B, Yan W. The structure-directing role of heterologous seeds in the synthesis of zeolite. *Green Energy Environ*

2024;9:792-801. DOI

40. Li J, Rong H, Chen C, et al. Synthesis optimization of SSZ-13 zeolite membranes by dual templates for N_2/NO_2 Separation. *Chem Res Chin Univ* 2022;38:250-6. DOI

41. Yam VWW, Li CK, Chan CL. Proof of potassium ions by luminescence signaling based on weak gold-gold interactions in dinuclear gold(I) complexes. *Angew Chem Int Ed Engl* 1998;37:2857-9. DOI PubMed

42. Moliner M, Rey F, Corma A. Towards the rational design of efficient organic structure-directing agents for zeolite synthesis. *Angew Chem Int Ed Engl* 2013;52:13880-9. DOI PubMed

43. Ding Y, Wang P, Tian YK, Tian YJ, Wang F. Formation of stimuli-responsive supramolecular polymeric assemblies via orthogonal metal-ligand and host-guest interactions. *Chem Commun* 2013;49:5951-3. DOI PubMed

44. Georgieva I, Danchova N, Gutzov S, Trendafilova N. DFT modeling, UV-Vis and IR spectroscopic study of acetylacetone-modified zirconia sol-gel materials. *J Mol Model* 2012;18:2409-22. DOI PubMed

45. Ke Q, Sun T, Cheng H, et al. Targeted synthesis of ultrastable high-silica RHO zeolite through alkali metal-crown ether interaction. *Chem Asian J* 2017;12:1043-7. DOI PubMed

46. Weigert FJ. Selective synthesis and equilibration of methylamines on sodium mordenite. *J Catal* 1987;103:20-9. DOI